International Journal of Applied Earth Observations and Geoinformation 117 (2023) 103220

Contents lists available at ScienceDirect

International Journal of Applied Earth Observations and Geoinformation

journal homepage: www.elsevier.com/locate/jag

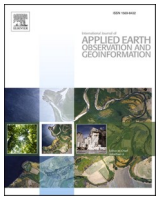

Less is more: Optimizing vegetation mapping in peatlands using unmanned aerial vehicles (UAVs)

Jasper Steenvoorden [a,*], Harm Bartholomeus [b], Juul Limpens [a]

[a] Plant Ecology and Nature Conservation (PEN), Wageningen University & Research, P.O. Box 47, 6700 AA Wageningen, The Netherlands
[b] Laboratory of Geo-information Science and Remote Sensing, Wageningen University & Research, P.O. Box 47, 6700 AA Wageningen, The Netherlands

ARTICLE INFO

Keywords:
Peatlands
Vegetation patterns
unmanned aerial vehicles (UAVs)
Heterogeneous landscapes
Remote sensing
Machine learning

ABSTRACT

1. Northern peatlands are inaccessible wetlands that serve important ecosystem services to humans, including climate regulation by storing and sequestering carbon. Unmanned aerial vehicles or drones are ideal to map vegetation and associated functions in these ecosystems, but standardized methods to optimize efficiency (highest accuracy with lowest processing time) are lacking.
2. We collected high-resolution drone imagery at three different altitudes (20 m, 60 m, and 120 m) of two Irish peatlands contrasting in pattern complexity and evaluated to what extent classification accuracy of vegetation patterns (microforms and plant functional types) changed using different flight altitudes, minimum segment size and training/testing sample size. We also analysed the processing time of all classifications to find the most efficient combination of parameters.
3. Classification accuracy was consistently high (>90 %) and estimated areas of both patterns were uniform among all flight altitudes, independent of pattern complexity. Minimum segment size and training/testing sample size were also important parameters affecting the efficiency of classifications. Total processing time from imagery capture to final map was 19–22 times faster with drone imagery at 120 m altitude than at 20 m, and seven times faster than at 60 m.
4. Our findings suggest that flying at the maximum legal altitude of 120 m is the most efficient approach for landscape-scale mapping of vegetation in peatlands or other ecosystems with similar short vegetation structure. We conclude that flying higher is always more efficient as long as the pixel size of drone imagery remains under the pixel size of the pattern under investigation.

1. Introduction

Northern peatlands (hereafter: peatlands) provide key ecosystem services to humans, like drinking water provision, flood control, water purification, biodiversity, and climate regulation through their natural ability to store disproportionally large amounts of carbon. Peatlands represent only about 2 % of the earths' surface (Xu et al., 2018), yet store between 472 and 620Gt of soil carbon (Yu et al., 2010), compromising more than one-third of all terrestrially stored soil carbon (Rydin & Jeglum, 2013), and>90 % of the global peatland carbon pool (Yu, 2011). Many peatland functions, including carbon sequestration, are strongly linked to vegetation structure (species composition, biomass, and spatial organisation), potentially enabling upscaling of this climate regulating service through vegetation patterns.

Peatland vegetation commonly exhibits characteristic spatial patterns in the landscape resulting from microtopographic irregularities called microforms, ranging from elevated moist hummocks, wet-moist lawns, wet depressions (hollows), to open water (Fig. 1). Because the plant species and plant functional types (PFTs) occurring along this micro-topographical gradient differ in functional traits, the distribution of microforms and their associated vegetation are commonly used indicators for peatland functioning, such as its hydrological condition and biogeochemical fluxes (Couwenberg et al., 2011; Lees et al., 2018; Schaepman-Strub et al., 2009). Yet, upscaling this information from

* Corresponding author.
E-mail address: jasper.steenvoorden@wur.nl (J. Steenvoorden).

https://doi.org/10.1016/j.jag.2023.103220
Received 7 November 2022; Received in revised form 11 January 2023; Accepted 1 February 2023
Available online 7 February 2023

plot-level to larger areas is complicated by the scale and heterogeneity of these patterns (Räsänen & Virtanen, 2019; Siewert & Olofsson, 2020), which range from 0.01 to 1 m for PFTs to 1–10 m for microforms, falling below the current spatial resolution of commercial satellites.

In recent years, remote sensing with unmanned aerial vehicles (UAVs) or drones has specifically gained much attention for its potential role in mapping and monitoring peatland vegetation and its functions. Drones can already capture the fine-scale heterogeneity of peatland microtopography and associated vegetation with unprecedented level of detail and will only evolve further and more rapidly in the upcoming years (Anderson & Gaston, 2013; Manfreda et al., 2018), making them an ideal bridge between field-based measurements and satellite remote sensing in these ecosystems. Besides, the distinct spectral differences between vegetation types along the micro-topographical gradient in combination with their relatively flat topography makes peatlands inherently suitable for mapping fine-scale vegetation patterns as it also

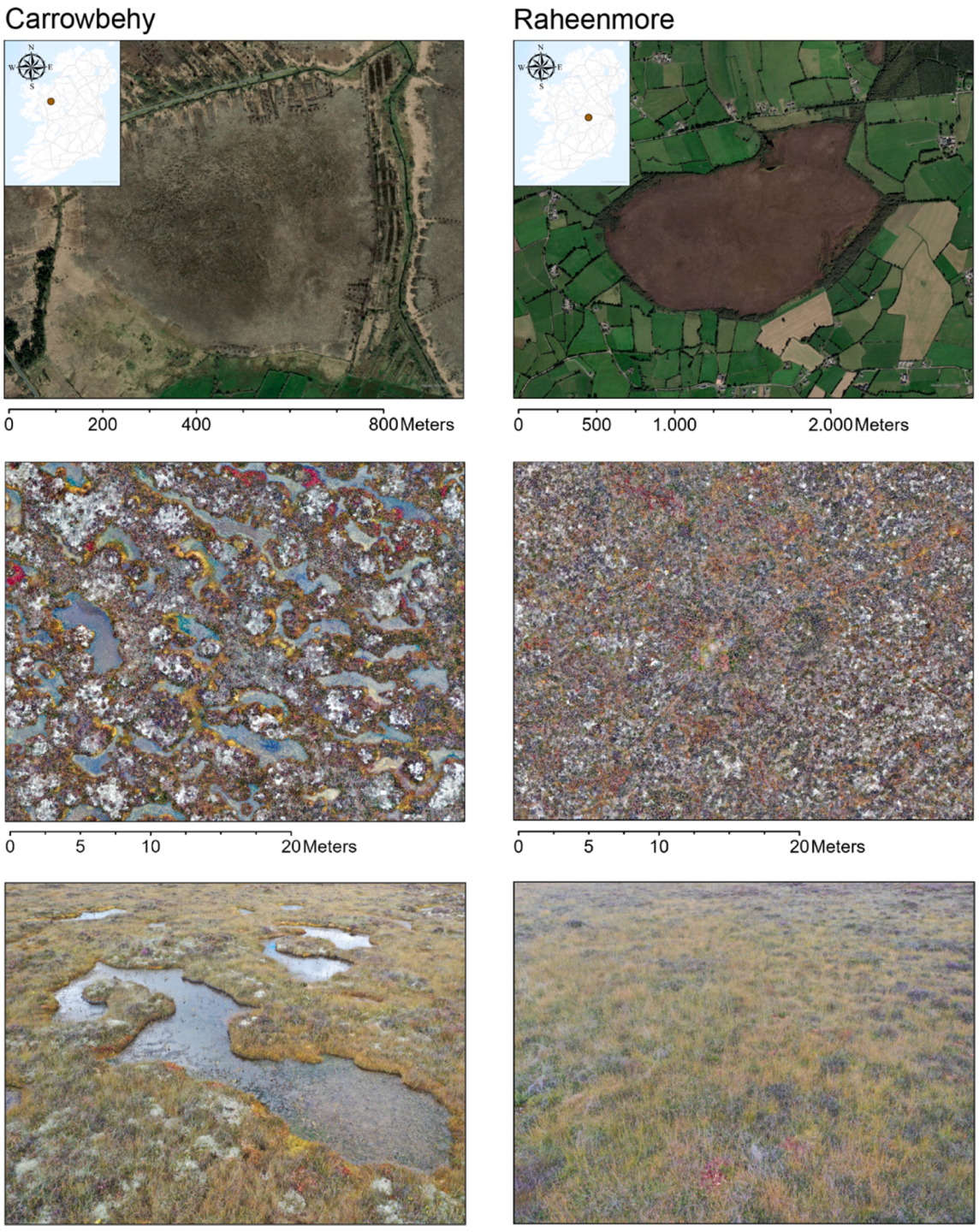

Fig. 1. Study area maps showing the characteristic vegetation patterns in the central areas of Carrowbehy (left) and Raheenmore (right). The top images show both studied peatlands as well as their location in Ireland (inset). Presented in the middle pictures are the vegetation patterns of Carrowbehy and Raheenmore as seen from drone imagery at 20 m altitude using a DJI Mavic 2 Pro. The bottom images show the vegetation patterns of both peatlands from images taken at 3 m altitude. Carrowbehy has a well-developed microform gradient ranging from open water pools to high hummocks, while vegetation patterns of Raheenmore have less developed microforms, largely dominated by hummocks and lawns and lacking permanent pools and hollows.

notably improves the accuracy of drone-derived photogrammetry products (Czapiewski, 2022; Lovitt et al., 2017). Multiple studies have highlighted the great potential of drone imagery for mapping fine-scale peatland vegetation patterns (e.g. Beyer et al., 2019; Bhatnagar et al., 2021; Lehmann et al., 2016; Palace et al., 2018; Räsänen et al., 2020a; Räsänen et al., 2019; Riihimäki et al., 2019; Steenvoorden et al., 2022). However, while promising, the relatively long processing times and limited spatial coverage of drones together with the unknown sensitivity of flight and image processing parameters to the complexity of spatial patterns currently hamper upscaling of the approach.

In this study, we sought to improve the efficiency of drone-based vegetation mapping (i.e. reducing total processing time without compromising on accuracy) by investigating the role of several flight and image processing parameters (flight altitude, training/testing sample size, and minimum segment size) on total processing time and accuracy of mapping peatland vegetation patterns. More specifically, we classified microforms and plant functional types in two peatlands with contrasting pattern complexity (heterogeneous vs homogeneous vegetation) using drone-derived remote sensing products taken at three different flight altitudes. We hypothesize that: 1) classification accuracy of vegetation patterns increases with larger sample sizes and segment sizes reflecting the real patchiness of vegetation patterns, 2) classification accuracy of vegetation patterns is independent of flight altitude, 3) classification accuracy increases in peatlands with more heterogeneous vegetation patterns, and 4) classification efficiency is significantly higher using imagery at 120 m altitude than imagery at lower altitudes.

2. Materials & methods

2.1. Study area

We selected two Irish ombrotrophic peatlands based on their contrasting levels of pattern complexity: well-developed heterogeneous patterns in Carrowbehy and less developed and more homogeneous patterns in Raheenmore (Fig. 1). Carrowbehy is a western raised bog complex of 343 ha that exhibits a very clear hummock-lawn-hollow pattern with occasional open water pools in the central and hydrologically most intact areas of the peatland (called the central ecotope; Fig. 1). While Carrowbehy has experienced moderate domestic peat cutting in its recent history, peat cutting has ceased here since 2003 (Fernandez et al., 2014), and it is currently a prime example of remaining ecohydrologically intact raised bogs in Ireland. Raheenmore is an eastern raised bog of 210 ha situated in the Irish Midlands and is one of the last surviving raised bogs in the eastern part of the country. In contrast with Carrowbehy, the central ecotope of Raheenmore has a less developed microtopography, lacking permanent pools and extensive hollows. Rather, the vegetation patterns of Raheenmore are more homogeneous and are largely dominated by hummocks interspersed with lawns filled with graminoids and some peat mosses (Fig. 1). Both peatlands are part of Irelands' Special Areas of Conservation (SAC's) network under the EU Habitats Directive (92/43/EE; Mackin et al., 2017; National Parks and Wildlife Service, 2018).

2.2. Drone imagery capture

We collected drone images of Carrowbehy and Raheenmore on 14 and 21 September 2021 respectively using a DJI Mavic 2 Pro drone with Hasselblad L1D-20c red-greenblue (RGB) colour sensor camera. We used no intrinsic camera parameters, except for the default camera calibration present in the EXIF information, which is limited to focal length (10.3 mm). All camera parameters were determined or optimized during the photogrammetric processing. We used DJI Ground Station Pro to design automated flights of 1 ha (or more depending on altitude) at an altitude of 20 m, 60 m, and 120 m above ground level for each peatland and a forward/side image overlap of 80/80, extending flight lines well beyond our region of interest to increase the number of overlapping images at the edges of our plot for use during photogrammetry. We decided upon using these altitudes because 120 m is the maximum legal flight altitude using consumer grade drones, 60 m is half of the maximum legal flight altitude and half the resolution of imagery at 120 m, and 20 m is an extremely low flight altitude reaching sub-centimetre spatial resolution. To allow for georeferencing of the stitched drone images at each flight altitude, we distributed four 30x40cm checkerboard ground control points around the edges of each 1 ha plot and measured their position using a Topcon HiPer HR real-time kinematic (RTK) and TopNET + global navigation satellite system (GNSS) with 1–3 cm accuracy. All flights were conducted within one hour of solar noon under fully cloudy conditions to minimize the effect of shade, where wind speeds varied between low to moderate wind speeds up to 19 km/h.

2.3. Pre-processing drone imagery

After all drone flights were conducted, we pre-processed all drone-derived imagery products before classifying vegetation patterns within each orthomosaic. First, we used *ortho*-mapping software in ArcGIS Pro 2.8.2 to colour balance the drone images and produce a stitched RGB orthomosaic of each flight, as well as to create a high-resolution Digital Terrain Model (DTM) with 5× pixel size of each orthomosaic (default setting) using the photogrammetric data contained within each individual drone image (Table S1). More specifically, we created the DTM using extended terrain matching, which is a feature-based stereo matching technique for generating high density point clouds. Hereafter, we georeferenced each orthomosaic using the ground control points and clipped the georeferenced orthomosaics to a rectangular polygon of 1 ha and 0.56 ha for Carrowbehy and Raheenmore respectively, because the orthomosaic of Raheenmore at 20 m altitude was only 75 × 75m.

Second, we grouped all pixels within each orthomosaic into segments (objects) using a mean-shift clustering algorithm based on similarity in spectral and spatial characteristics of the raster image. To calibrate the optimal minimum segment size for classification of microforms and plant functional types (PFTs) in our study, we carried out this segmentation fourteen times for both patterns in both peatlands (total of 60 segmentations) using the imagery at 120 m altitude (Table 1). We started with a minimum segment size of 0.01 m^2 ground area (0.1 × 0.1 m) and increased minimum segment size by 0.05 × 0.05 m after every iteration of the classification algorithm up to a minimum segment size of 0.5625 m^2 (0.75 × 0.75 m). We only performed this analysis at 120 m because the ground area is independent of flight altitude, and we argue that repeated segmentations at lower altitudes would therefore likely lead to very similar results.

Third, we detrended each DTM by fitting a second-order polynomial function through the elevation points in the DTM, and subsequently subtracted the DTM from the fitted trend function. This detrended DTM represents relative micro-topographical differences within the orthomosaic more realistically and was needed because the DTM of each orthomosaic was slightly sloping downwards from the centre to the margin of the peatlands.

Lastly, we calculated several RGB-derived vegetation colour indices as additional predictor variables in the classification of both microforms and PFTs to further emphasise spectral differences between vegetation classes. Ultimately, we employed a total of 25 predictor variables in the classification of both microforms and PFTs, consisting of the mean and standard deviation of RGB values, mean of the Hue-Saturation-Value colour model, ten vegetation colour indices combining two or more RGB bands, elevation (minimum, maximum, and mean) and three shape metrics (pixel count, rectangularity, and compactness), computed separately for all segments in each orthomosaic (Table S2).

2.4. Ground truth data

We divided vegetation patterns in our study into microforms and

Table 1
overview of the imagery that was used to evaluate each hypothesis of the study. First, we used the imagery of both Carrowbehy (heterogeneous) and Raheenmore (homogeneous) at 120 m altitude to calibrate the optimal minimum segment size for the study. We then used the results of the sensitivity analysis of training/testing sample size for Carrowbehy at 120 m altitude to adjust the training/testing sample size for Raheenmore. Afterwards, we applied these calibrated image processing parameters to all subsequent classifications for both peatlands. A check mark (green) is used to indicate that a dataset was used during analysis for evaluating a specific hypothesis, whereas a cross (red) indicates that a dataset was not used in analysis for evaluating a specific hypothesis.

Hypotheses	Carrowbehy (heterogeneous)			Raheenmore (homogeneous)		
	20m	60m	120m	20m	60m	120m
Hypothesis 1 (Sensitivity analyses)	×	×	✓	×	×	✓
				Adjust total training/testing sample size of Raheenmore		
	Apply calibrated optimal minimum segment size to all subsequent classifications					
Hypothesis 2 (Flight altitude)	✓	✓	✓	✓	✓	✓
Hypothesis 3 (Pattern complexity)	✓	✓	✓	✓	✓	✓
Hypothesis 4 (Classification efficiency)	✓	✓	✓	✓	✓	✓

PFTs because they are two common conceptualizations used in mapping vegetation patterns and functions in peatlands. Hereafter, we further subdivided each vegetation pattern into classes based on drone-visible indicator species (or the lack thereof) and their associated position along the micro-topographical gradient as seen from the newly developed orthomosaics. Microforms were subdivided into three classes: 1) hollow, 2) lawn, and 3) hummock (Table S3), while PFTs were subdivided into five classes: 1) peat moss, 2) shrub, 3) graminoid, 4) lichen, and 5) water/bare peat (Table S3).

For classification of microforms, we initially created 500 randomly placed points within each orthomosaic for Carrowbehy and used the highest resolution orthomosaic at 20 m altitude as a reference dataset to create training/testing samples for use in classification. The geographical locations of these point measurements were then linked to the values of the predictor variables within the computed segment by which they were contained to develop the full training/testing dataset. We increased total training/testing sample size for microforms to 625 points (375 hummock, 150 lawn, and 100 hollow) by randomly adding new points until we reached a rounded-out approximation of area-proportional allocation of training/testing samples for Carrowbehy. For classification of PFTs, we instead adopted a targeted sampling approach, where we placed 100 points per PFT per orthomosaic for Carrowbehy (500 total; five PFTs) to prevent underrepresentation of uncommon PFTs in each orthomosaic.

To evaluate the effect of training/testing sample size on classification accuracy, we performed a sensitivity analysis on the training/testing samples during classification of microforms for Carrowbehy at 120 m altitude where we systematically reduced the proportion of total training/testing samples from 100 % to 10 % with steps of 10 %. The results of this sensitivity analysis were then used to adjust the total training/testing sample size for classification of microforms for Raheenmore to a reduced sample size that still had consistent accuracy compared to the full sample size (see also 3.1.2; Table 1). For PFTs we used the same sensitivity analysis as for microforms, after which we also adjusted the total training/testing sample used for classification of PFTs for Raheenmore to the reduced sample size where classification accuracy remained consistent (see also 3.1).

2.5. Vegetation pattern classification

We classified vegetation classes of each pattern based on selected segments using the training/testing samples within each orthomosaic in combination with the ensemble classifier Random Forest (Breiman, 2001) using Python's Scikit-learn module (Pedregosa et al., 2011) with the 25 predictor variables as input. We used Random Forest as it is a robust and interpretable machine learning algorithm with little demand on computational power (Belgiu & Drăgu, 2016). To fit the Random Forest models, we first removed redundant predictor variables from the whole training/testing sample of each orthomosaic using the Boruta feature-selection algorithm (Kursa & Rudnicki, 2010). We then split the training/testing samples for each orthomosaic using stratified K-fold cross-validation (CV) with a ratio of 80:20 for training versus testing (analogous to 5-folds) because it minimized variance of CV model accuracy in our study as compared to repeated K-Fold cross-validation or a larger number of folds (Jiang & Wang, 2017). We kept hyperparameters of the Random Forest classifier at default values as accuracy improvements through hyperparameter tuning were negligible (less than1 %). Classification accuracy per vegetation class as well as final classification accuracy of each orthomosaic were computed by averaging precision, recall, and F1-score over all folds in the Random Forest model using the testing samples. An average value of 1 then indicates a perfect prediction, while any value in between 0 and 1 (or 0–100 %) indicates the probability that a testing sample is correctly classified. We classified all segments within each orthomosaic by taking the most frequently classified vegetation class for each segment over all folds. Lastly, we retrieved an overall ranking of variable importance for each classified image by computing the Gini importance, which we used as it is a commonly used measure for variable importance in peatland studies (Behnamian et al., 2017; Millard & Richardson, 2015). Because variable importance rankings for each plot varied between Random Forest model runs (i.e. folds), we averaged Gini importance over all folds to receive more stable mean importance values for each classification (Behnamian et al., 2017). In cases where a predictor variable was removed through Boruta, variable importance was set to 0.

2.6. Stratified estimation of mapped class areas

After each orthomosaic was classified, we used the confusion matrix and mapped class area (m^2) from the classification of each orthomosaic to estimate accuracy and quantify uncertainty of the mapped class areas using stratified estimation (Olofsson et al., 2013, 2014). More specifically, we used the ratio between true positives, false positives, true negatives, and false negatives for each class within the confusion matrix in combination with the mapped area of each class to compute their error-adjusted area estimates and confidence intervals as well as recalculating the accuracy measures and confidence intervals hereof using the stratified area estimates. Stratified estimation represents the uncertainty in mapped areas due to misclassifications more realistically, whereas solely using sample counts from the confusion matrix as means of assessing classification accuracy can severely underestimate or overestimate the true accuracy and area of vegetation classes. This is crucial, especially since variability in mapped class area estimates resulting from misclassifications could have cascading effects when for instance developing models that link vegetation patterns to functions such as carbon fluxes (Olofsson et al., 2013). Stratified estimation is a transparent and statistically robust approach to assess accuracy and estimate mapped areas of vegetation classes, and therefore allows for more effective use of drone imagery products in later analyses. Besides, by taking this uncertainty into account, it allowed for better comparison of the consistency between mapped areas of each vegetation class at the different altitudes used in this study. A workflow of our full research methodology can be seen in Figure S1.

3. Results

3.1. Sensitivity analyses

3.1.1. Optimal minimum segment size

Before classifying microforms and plant functional types (PFTs) at all three flight altitudes, we first classified both vegetation patterns at 120 m altitude at both peatlands using a total of fourteen different minimum segment sizes ranging from 0.1 m to 0.75 m to determine the optimal minimum segment size for classification of each vegetation pattern. This analysis showed that classification accuracy is highly dependent on the minimum size of the segments within an orthomosaic, and that

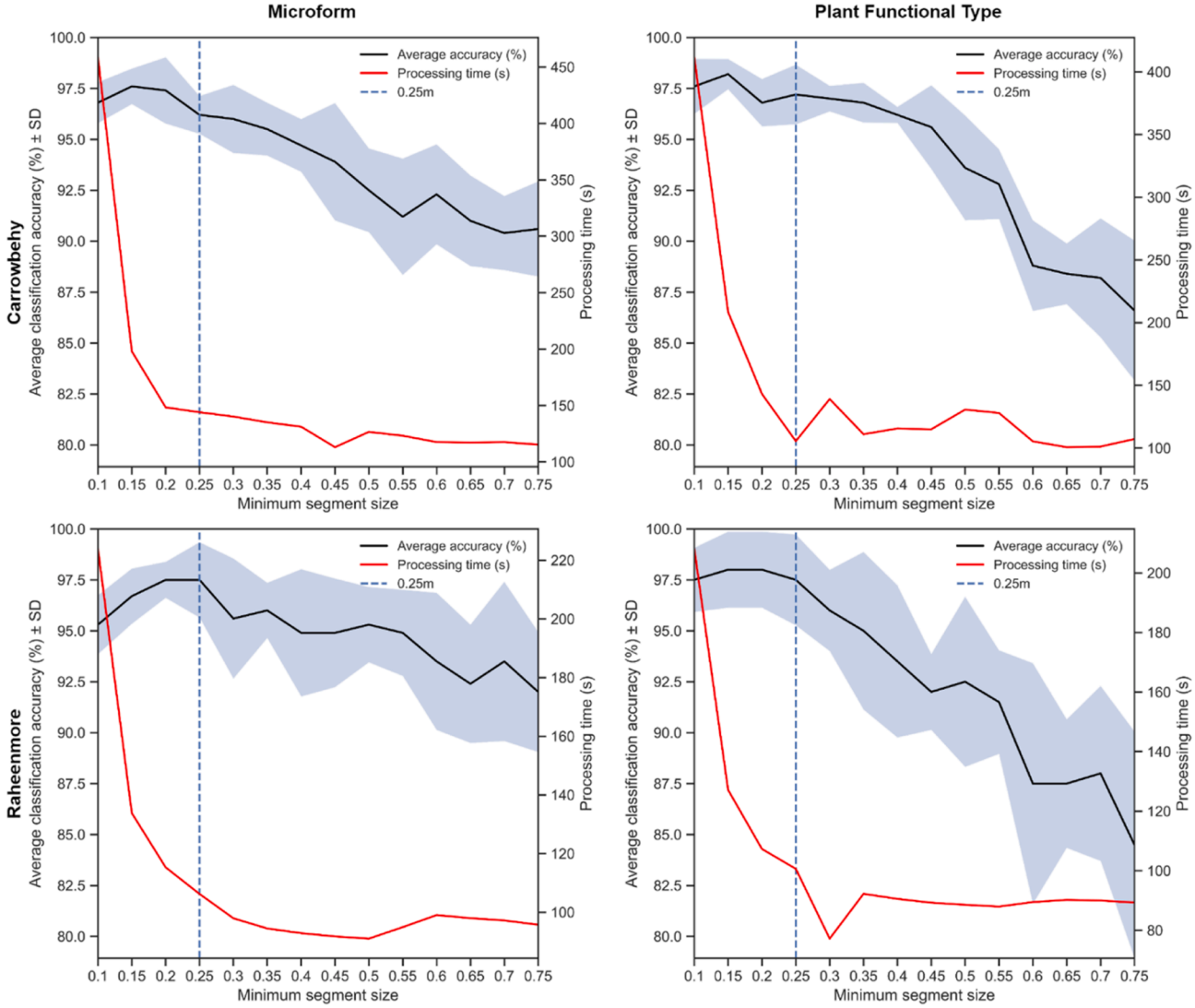

Fig. 2. relationship between average classification accuracy and processing time of microforms (left) and plant functional types (right) for heterogeneous Carrowbehy (top) and homogenous Raheenmore (bottom). The black line represents the average classification accuracy over five folds using stratified K-fold cross-validation (black), with the blue shaded area indicating the standard deviation. The red line indicates the classification time (i.e. time total time for segmentation, training of Random Forest models, and classification of orthomosaic). The dashed vertical line indicates the minimum segment size of 0.25 m. (For interpretation of the references to colour in this figure legend, the reader is referred to the web version of this article.)

minimum segment size also strongly influences classification time. Overall, classification accuracy and variance were comparable for both peatlands and for both vegetation patterns until a minimum segment size of 0.25 m (Fig. 2; Table S4–S7), after which accuracy started dropping and variance started increasing notably up until a minimum segment size of 0.75 m. In addition, reductions in processing time were largest from 0.1 to 0.25 m, whereas reductions in processing time from 0.25 to 0.75 m were only twelve seconds on average for all four classifications (Table S4–Table S7; Fig. 2). These results highlighted that a minimum segment size of 0.25 m is most efficient independent of the studied vegetation pattern (microform or PFT) or pattern complexity, and we therefore decided to use a minimum segment size of 0.25 m for all further analyses.

3.2. Training/testing sample size

After determining an optimal minimum segment size of 0.25 m, we performed our sensitivity analysis on the training/testing sample size for Carrowbehy. For microforms, the sensitivity analysis highlighted that classification accuracy and variance of CV model accuracy were consistent until 40 % of the total training/testing sample size remained (Table S8; Fig. 3). The sensitivity analysis for PFTs in Carrowbehy showed that classification accuracy and variance of CV model accuracy were consistent until 50 % of the total training/testing sample size remained (Table S9; Fig. 3). These results underscored that total training/testing sample sizes of 625 and 500 for microforms and PFTs respectively were more than adequate to reach consistent classification accuracies for Carrowbehy. Consequently, we used reduced total training/testing sample sizes as ground truthing data during classification of microforms and PFTs for Raheenmore. Here, we created only 250 random points (40 % of 625 points) of microforms within each orthomosaic and rounded out these points to a total training/testing sample size of 275 points (200 hummock and 75 lawn points). For PFTs, we placed only 50 points per PFT (200 in total; four PFTs) per orthomosaic in Raheenmore as training/testing samples for use in classification.

3.3. Vegetation pattern classifications

3.3.1. Microform classifications

Classified images of microforms showed average accuracies of well over 90 % at all flight altitudes, where the lowest accuracy was 95.2 % (Carrowbehy at 60 m) and the highest accuracy was 97.8 % (Raheenmore at 20 m). Besides, classification reports for each classified orthomosaic highlighted that accuracies per microform were also generally very high, with accuracies reaching at least 90 % in all cases (Table S10). Misclassifications in Carrowbehy most often occurred between lawn and hummocks, but occasionally also between hummock and hollow (Table S15), likely explained by occasional similarities in spectral reflectance between species of different microforms (see also discussion 4.1). In Raheenmore, only hummock and lawn were present, which were therefore always misclassified as each other. Analysis of variable importance emphasized that both vegetation colour indices and elevation predictor variable categories were always important in classification of microforms for both peatlands, whereas RGB values and shape metrics were hardly ever important or even included the Random Forest models after feature selection with Boruta (Figure S3). The high classification accuracies of all microforms in both peatlands show that the detectability and mappability of microforms in our study was extremely good independent of pattern complexity.

Mapped class areas for each classification emphasized that hummock was by far the largest class at all three altitudes for both peatlands (Fig. 4; Fig. 5), followed by lawn and hollow, which both occurred approximately in equal amounts in all peatlands (Fig. 4). After stratified estimation, error-adjusted areas for each microform changed slightly in each peatland (Fig. 4; Table S12), but the substantially overlapping confidence intervals for estimated areas of all microforms underline that these values are not significantly influenced by flight altitude. These findings signify that carrying out drone flights below 120 m altitude (2.7 cm pixel size in our study) provided no benefit to classification accuracy of microforms.

3.4. Plant functional type classifications

Like microforms, classified images of plant functional types (PFTs) also showed average accuracies of well over 90 % at all flight altitudes.

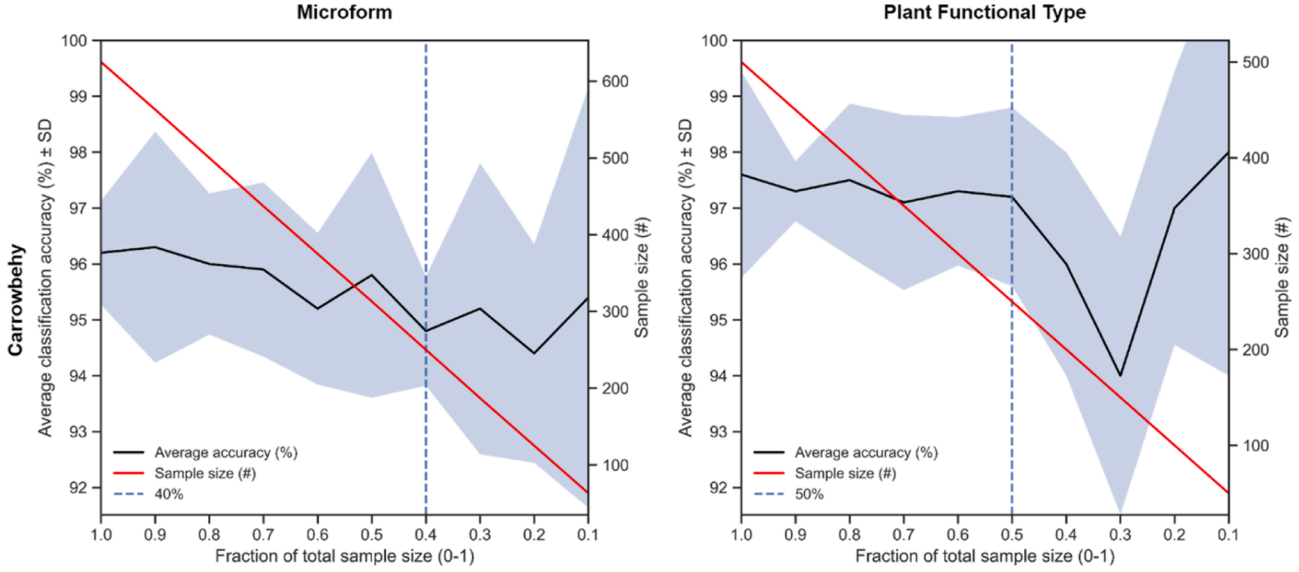

Fig. 3. relationship between total sample size (and fraction of total sample size) on the accuracy of classifications of microforms (left) and plant functional types (right) for Carrowbehy using a minimum segment size of 0.25 m. The black line represents average classification accuracy over five folds using stratified K-fold cross-validation, with the blue shaded area indicating the standard deviation. The red line indicates total sample size, and the vertical dotted line highlights the minimum fraction for consistent classification results (40 % for microforms and 50 % for plant functional types). (For interpretation of the references to colour in this figure legend, the reader is referred to the web version of this article.)

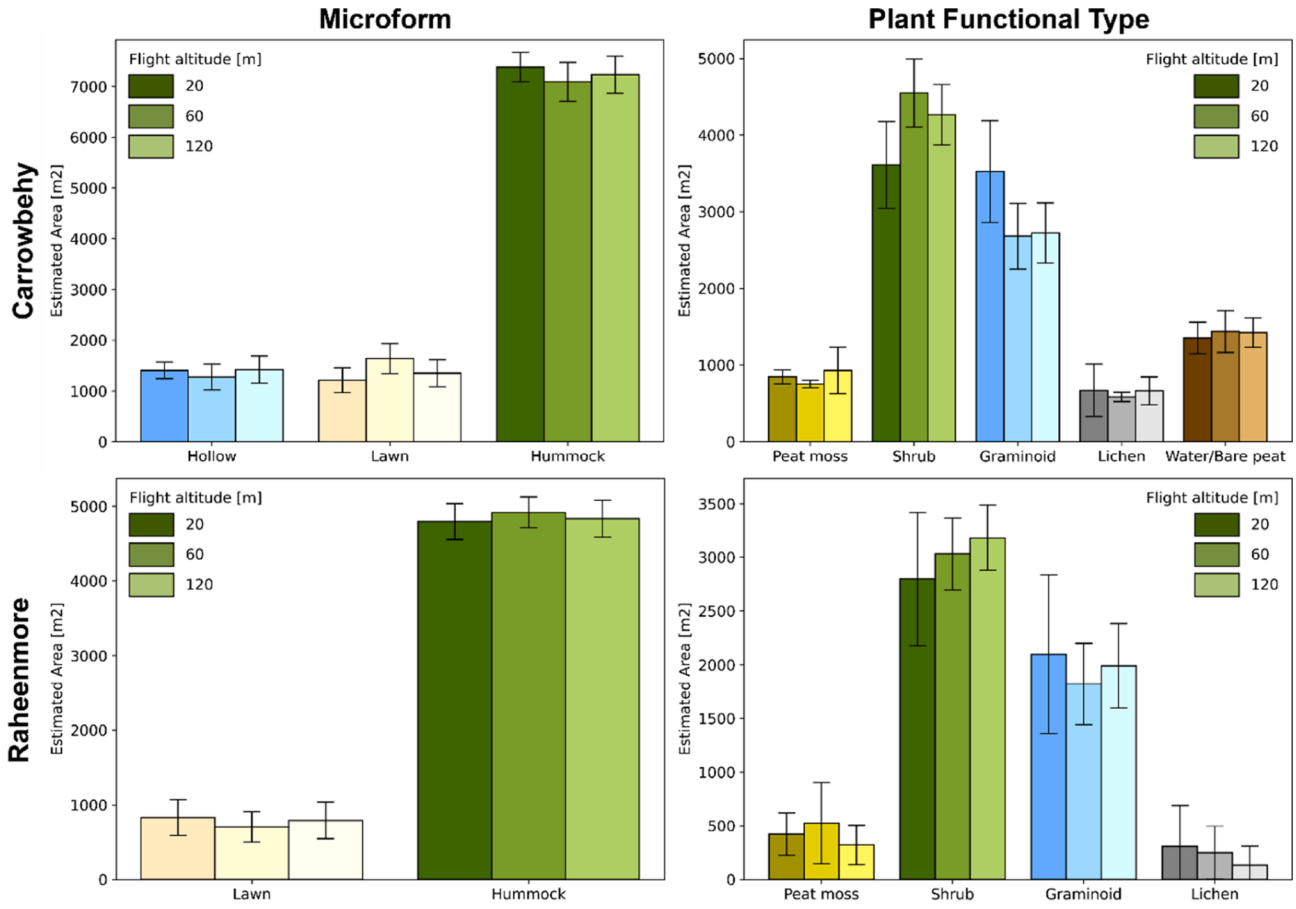

Fig. 4. overview of estimated areas (m^2) with confidence intervals for classification of microforms (left) and plant functional types (right) at all three altitudes (20 m, 60 m, and 120 m) for both studied peatlands with varying pattern complexity: Carrowbehy (top, heterogeneous) and Raheenmore (bottom, homogeneous). Bars for each vegetation class of each pattern represent estimated areas at 20 m (left), 60 m (center), and 120 m (right).

Here, lowest classification accuracy was 92.5 (Raheenmore at 20 m) and the highest accuracy was 97.5 (Raheenmore at 120 m). Classification reports for each classified orthomosaic showed that accuracies per PFT were also generally very high (Table S11), with accuracies reaching at least 90 % for all classes but graminoid at 20 m for both Carrowbehy (87.4 %) and Raheenmore (84.6 %), highlighting that graminoid was most difficult to classify at low flight altitudes. Misclassifications of PFTs in both Carrowbehy and Raheenmore most often occurred between graminoid and shrub and between graminoid and lichen (Table S15), likely also explained by occasional similarities in spectral reflectance between classes (see also discussion 4.1). Variable importance for classifications of PFTs differed strongly when compared to those of classifications of microforms in both peatlands. Here, mean RGB values, Hue-Saturation-Value colour model values and vegetation colour indices were the most important predictor variable categories, whereas elevation was hardly ever of importance in the Random Forest models (Figure S3). This is likely caused because the same PFTs can occur at multiple locations along the micro-topographical gradient as well as in multiple microforms. Based on the consistently high classification results of PFTs for both peatlands, we argue that pattern complexity has no effect on the detectability of PFTs in our study.

Mapped class areas for each classification highlighted that shrub and graminoid were the most dominant PFTs in each peatland, followed by peat moss, lichen, and water/bare peat (occurred in Carrowbehy only; Table S13; Fig. 4; Fig. 5). After stratified estimation, error-adjusted areas for each PFT changed slightly in each peatland. The confidence intervals show that ranges in error-adjusted areas for shrub and graminoid are highest in both locations at 20 m because of their reduced classification accuracy, and that ranges in error-adjusted areas are also large for lichen in Raheenmore because lichen was sometimes classified as graminoid, which occurred in large proportions. Nevertheless, the confidence intervals for estimated areas of PFT classes for all altitudes still overlap substantially, highlighting that these estimated areas are also consistent at all three altitudes for both peatlands (Table S13; Fig. 4). These results also signify that drone flights below 120 m altitude provide no benefit to classification accuracy of PFTs, and that classification accuracy even improves at higher altitudes instead because of reduced misclassifications between shrub and graminoid.

3.5. *Classification efficiency*

To analyse the efficiency of mapping microforms and plant functional types in our study using drone imagery, we summarized total image capture and processing time for the imagery at each altitude using 80/80 forward/side overlap and a minimum segment size of 0.25 m (Fig. 6; Table S14). Here, we assumed that classification accuracy of both vegetation patterns was consistent at all three altitudes for both peatlands based on the largely overlapping confidence intervals of estimated areas for each class within a vegetation pattern. Total processing time from imagery capture to final map was approximately seven times faster at 120 m altitude than at 60 m and between 19 and 22 times faster than at 20 m for both vegetation patterns in both peatlands (Fig. 6). A considerable amount of this processing time at lower altitudes was spent capturing and pre-processing the drone imagery (Fig. 6; Table S14), which is most likely caused by the large number of pixels per area in 20 m imagery as opposed to imagery at 60 m and 120 m (Table S1). We therefore argue that aside from other flight and processing parameters, flying at the maximum legal flight altitude of 120 m

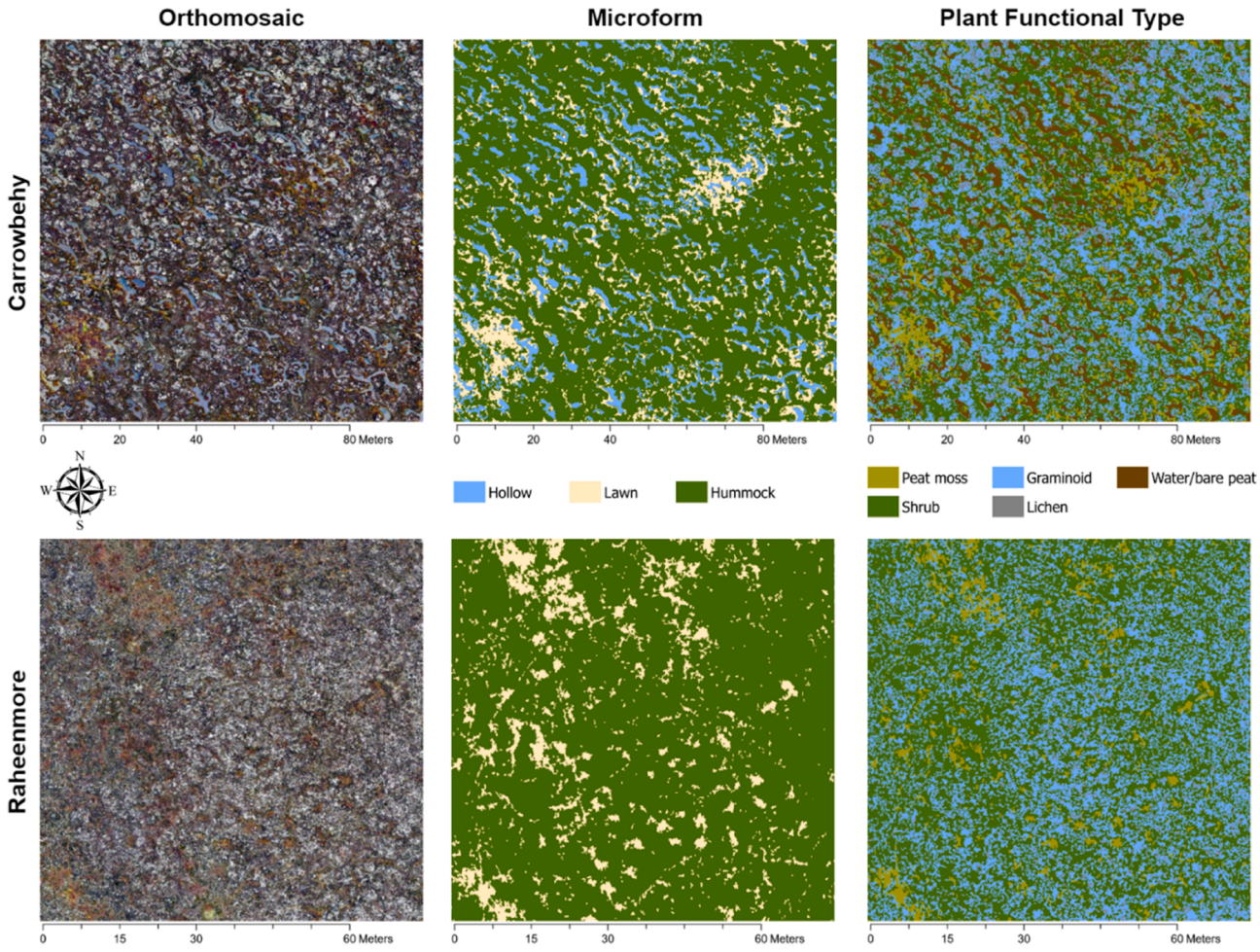

Fig. 5. maps showing the classification results at 120 m altitude for both studied peatlands with varying pattern complexity: Carrowbehy (top, heterogeneous) and Raheenmore (bottom, homogeneous). Represented for each peatland are the orthomosaic at 120 m altitude (left), classified map of microforms at 120 m altitude (centre), and classified map of plant functional types at 120 m altitude (right).

is by far the most efficient approach for mapping peatland vegetation patterns, at least in our study.

4. Discussion

4.1. Consistency of peatland vegetation pattern classifications

We found that classification accuracy of vegetation was not affected by flight altitude up to 120 m, pattern complexity or spatial scale of the pattern (microforms vs plant functional type). We attribute the high consistency of the classification accuracy to three main factors: 1) the high spectral separability of peatland vegetation, 2) the role of topographical data on class separability, and 3) optimization of spatial resolution and segmentation scale. While drones may be particularly suited for landscape-scale vegetation mapping of open, tree-less peatlands, the insensitivity of classification results to pattern complexity suggests that our results are not limited to these ecosystems. Instead, we think drones can as efficiently be used for mapping vegetation in other ecosystems with similar short vegetation structure, such as moorlands, heathlands, or tundra, albeit by having slightly different data and resolution requirements than peatlands.

4.2. Spectral separability

The environmental gradients associated with microtopography in peatlands strongly determine their species composition. Microforms represent a distinct set of species and PFTs that are adapted to the biogeochemical and hydrological conditions of that microform, which act as filters on plant traits and associated spectral properties (Schaepman-Strub et al., 2009). As a result, the spectral reflectance of the PFTs dominating these species assemblages often differ markedly among another (see also Fig. 1; Table S3). The high spectral separability of vegetation classes at the time of our study may also explain why classification accuracy was rather insensitive to training/testing sample sizes, which was against our hypothesis. As spectral separability is co-determined by plant phenology (e.g. Palace et al., 2018; Räsänen et al., 2020a), our results may be linked to the end-of-season image capture.

4.3. Topographical data

In cases where different microforms contained PFTs with similar spectral signatures, including topographical data in the classification improved separability between vegetation classes. Indeed, the elevation predictor variables were always included after feature selection with Boruta, and improved classification accuracy of microforms in both peatlands (Figure S3). These results align with other recent studies in peatlands, who have shown that combining spectral data with topographical data can improve the accuracy of classification in vegetation studies quite substantially (e.g. Harris & Baird, 2019; Moore et al., 2019; Räsänen et al. (2020a,b)).

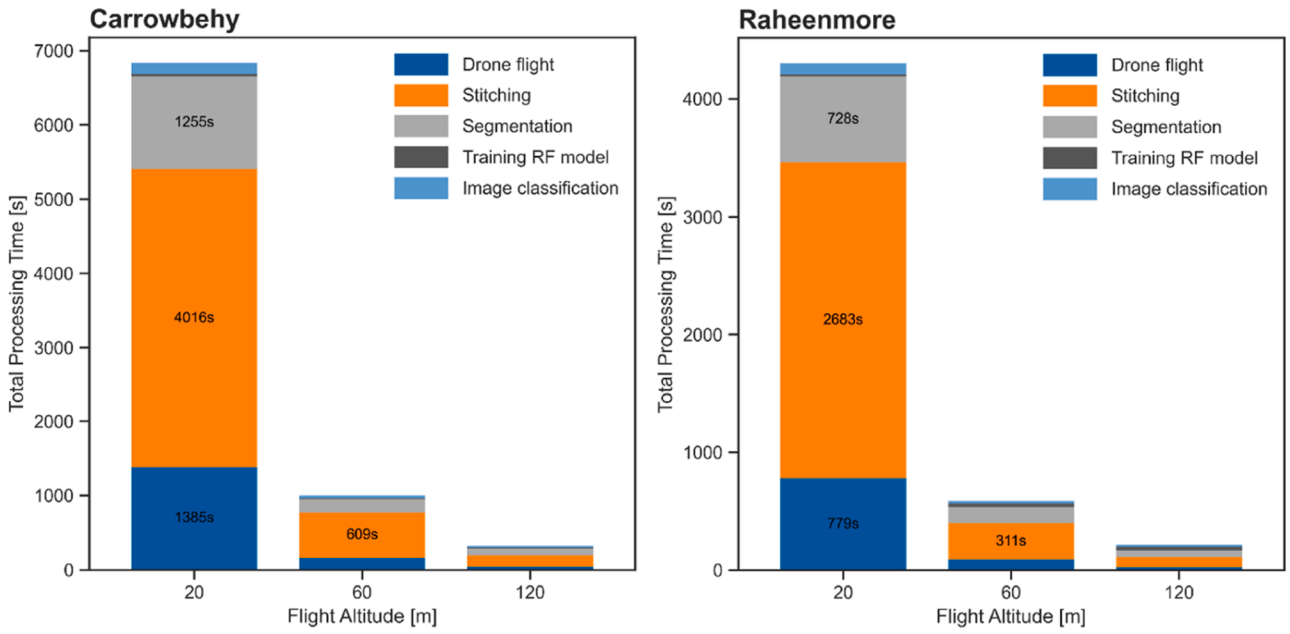

Fig. 6. stacked bar plots highlighting the total processing time for different processes carried out during classification of microforms and plant functional types at three altitudes (20 m, 60 m, and 120 m) in two peatlands (Carrowbehy and Raheenmore) with contrasting complexity. Because processing times of different patterns within a peatland were near equal, the presented processing times are averaged over the classifications of microforms and plant functional types for that specific peatland and altitude. Processing times are presented in chronological order from image capture to final map. Bars with processes that compromised less than 300 s are not labelled for visual clarity.

4.4. Spatial resolution and segmentation scale

The results of our study show that classification success depended strongly on evaluation of both the spatial resolution of input imagery and the choice of segmentation parameters, which is in line with other peatland mapping studies (e.g. Räsänen & Virtanen, 2019; Virtanen & Ek, 2014). Because the spatial resolution of our drone imagery already significantly surpassed the minimum size of our investigated vegetation patterns even at 120 m altitude (2.7 cm in our study), this led to a trade-off during segmentation. Here, higher segment sizes would allow for mapping of larger features but may miss smaller and clustered patches, whereas lower segment sizes can detect small and clustered features but may also lead to noise during classification by introducing heterogeneity within vegetation classes (Räsänen & Virtanen, 2019), for instance by attributing different plant parts such as stems, leaves, flowers and even canopy shadow to different segments. In our study, higher spatial resolutions and lower segment sizes were not always better in distinguishing between vegetation classes, whereas efficiency was improved notably once spatial resolutions and segment sizes reflected the real scale of the vegetation patterns under investigation. Our sensitivity analysis showed that microforms and PFTs had an optimal minimum segment size of about 0.25 m, which is likely low enough to identify smaller patches but not so small that vegetation classes show notable internal heterogeneity.

4.5. Improving mapping of fine-scale vegetation patterns

4.5.1. Choosing scales of interest

While we found a minimum segment size of 0.25 m to optimize classification accuracy in this study, this is by no means the gold standard for the segmentation scale of microforms and PFTs because the size and shape of patterns can vary between vegetation classes within a peatland, as well between vegetation patterns among peatlands. For instance, while hummocks are generally large and compact, lawns and hollows are often smaller and more elongated. Besides, whereas hummocks are often compromised by multiple PFTs, lawns can be inhabited homogeneously by peat mosses. Consequently, the difficulty of segmentation is that there is often no way to know which segmentation approach produces the best classification results until the classification is carried out. For this reason, we argue that one should first investigate the size and shape at which ecologically meaningful vegetation patterns exist in their study area, and then compare the effect of various relevant segmentation scales on classification efficiency to choose the most optimal segmentation scale for that site or goal. Here, one could also make use of multi-resolution segmentation where multiple segmentation scales are used for delineation of patches of different vegetation classes (Blaschke et al., 2014; Dronova, 2015), although this is more difficult to implement in a classification algorithm.

4.6. Training/testing sample size and allocation

The results of our classifications showed consistent accuracy metrics even with only 40–50 % of the original training/testing sample size, illustrating that defining an 'optimal' training/testing sample depends on a specific research or accuracy objective. For instance, to improve classification accuracy of Random Forest models, training/testing sample sizes should be as large as possible, and randomly distributed or at least created in a manner that allows for approximate area-proportional allocation of samples (Colditz, 2015; Millard & Richardson, 2015). However, to achieve acceptable standard errors for estimated accuracy metrics and area estimates, Olofsson et al. (2014) recommend that one should shift the sampling strategy slightly away from area-proportional allocation by increasing the sample size of uncommon classes (but not until equal allocation is reached). While we did not actively test the effect of sample size allocation on estimated accuracy metrics, we did see that variance of area estimates decreased notably in our study when total training/testing sample size was increased. Consequently, if the goal is to receive an accurate classification, 'as large as possible' means increasing a randomly distributed sample size up until a certain point where additional samples do not further improve accuracy. If the goal is instead to reduce standard errors of accuracy and area estimates of mapped vegetation classes, one should systematically evaluate the

potential outcome of a specific training/testing sample size and sample allocation on their values until a desired confidence interval is reached. In either case, the decision is based on the specific research purpose or accuracy objective.

4.7. Less is more

Our results suggest that classifications remain consistent as long as the pixel size of drone imagery remains under the pixel size of the investigated pattern. Consequently, efficiency of mapping fine-scale vegetation patterns can likely be improved further by using drones with lower resolution sensors because these reduce overall flight time per area, total image capture, and processing time using otherwise identical flight parameters. Besides, several recent drone studies have successfully mapped vegetation patterns in northern peatlands and tundra ecosystems using lower resolution imagery between 3 and 16 cm (Beyer et al., 2019; Palace et al., 2018; Räsänen et al., 2019; Räsänen & Virtanen, 2019; Siewert & Olofsson, 2020), highlighting the possibilities of further reducing spatial resolution without compromising on accuracy. Lower spatial resolution imagery could potentially also be obtained by flying at higher altitudes, but current legislation in most countries prohibits drone flying above 120 m altitude.

4.8. Linking patterns to functions

Because peatland vegetation patterns play such a key role in the carbon balance of peatlands, a next step in drone imagery analyses will be to link vegetation patterns to carbon related functions. Several studies have already started such analyses for carbon fluxes (e.g. Kelly et al., 2021; Lees et al., 2018; Lehmann et al., 2016; Moore et al., 2019), belowground C stocks (Lopatin et al., 2019), biomass (e.g. Cunliffe et al., 2020; Fraser et al., 2016; Räsänen et al., 2020b), and groundwater tables (Kalacska et al., 2018; Rahman et al., 2017). However, the major challenge for mapping vegetation patterns and functions in peatlands as well as other ecosystems with similar short vegetation structure is that drones will most likely never compete with the spatial coverage of commercial satellite imagery because of both technological and legislative limitations. Besides, these ecosystems are often large, continuous, isolated, and inaccessible. Consequently, nested drone-satellite approaches – where fine-scale drone imagery products are used to train larger-scale commercial satellite imagery (Bhatnagar et al., 2021; Riihimäki et al., 2019) – will likely become a necessity to be able to accurately and realistically upscale the fine-scale heterogeneous nature of peatland vegetation and their functions to the large scale at which they occur in the landscape. We think this factor is crucial and in need for further assessment in order to develop methods that can map and quantify peatland functions at regional and global scale. This will help us to better understand the vulnerability of global peatland carbon to predicted changes in climate and land-use in the 21st century.

5. Conclusion

The results of our study highlight the consistency of mapping fine-scale peatland vegetation patterns across multiple legal flying altitudes and in peatlands with both high and low pattern complexity. Based on these findings, we conclude that using otherwise identical flight and image processing parameters, flying at the maximum legal flight altitude of 120 m is always significantly more efficient than flying at lower altitudes as long as the pixel size of drone imagery remains under the pixel size of the pattern under investigation. When flying at 120 m altitude, drones are extremely well-suited for landscape-scale mapping of fine-scale vegetation patterns because of the flexibility and ease by which they can accurately and efficiently collect and process very high-resolution spectral and topographical data into vegetation pattern maps over relatively large areas. However, given the spatial characteristics of peatlands worldwide, we urge development of nested drone-satellite approaches to allow for further upscaling of vegetation patterns and their functions to the regional and global scale.

CRediT authorship contribution statement

Jasper Steenvoorden: Conceptualization, Methodology, Software, Formal analysis, Writing – original draft, Visualization. **Harm Bartholomeus:** Methodology, Writing – review & editing, Validation. **Juul Limpens:** Conceptualization, Methodology, Supervision, Writing – review & editing.

Declaration of Competing Interest

The authors declare that they have no known competing financial interests or personal relationships that could have appeared to influence the work reported in this paper.

Data availability

All data will be uploaded to the open source data repository DANS upon publication.

Acknowledgements

We thank the Irish National Parks and Wildlife Service (NPWS) for providing access to the studied peatlands, Matthijs Schouten for information and knowledge on the distribution and characteristics of fine-scale vegetation patterns in Irish peatlands, and Rúna Magnusson and Daniel Kooij for valuable discussions regarding the methodology of the study.

Appendix A. Supplementary material

Supplementary data to this article can be found online at https://doi.org/10.1016/j.jag.2023.103220.

References

Anderson, K., Gaston, K.J., 2013. Lightweight unmanned aerial vehicles will revolutionize spatial ecology. Front. Ecol. Environ. 11 (3) https://doi.org/10.1890/120150.

Behnamian, A., Millard, K., Banks, S.N., White, L., Richardson, M., Pasher, J., 2017. A Systematic Approach for Variable Selection with Random Forests: Achieving Stable Variable Importance Values. IEEE Geosci. Remote Sens. Lett. 14 (11) https://doi.org/10.1109/LGRS.2017.2745049.

Belgiu, M., Drăgu, L., 2016. Random forest in remote sensing: A review of applications and future directions. ISPRS J. Photogramm. Remote Sens. 114 https://doi.org/10.1016/j.isprsjprs.2016.01.011.

Beyer, F., Jurasinski, G., Couwenberg, J., Grenzdörffer, G., 2019. Multisensor data to derive peatland vegetation communities using a fixed-wing unmanned aerial vehicle. Int. J. Remote Sens. 40 (24), 9103–9125. https://doi.org/10.1080/01431161.2019.1580825.

Bhatnagar, S., Gill, L., Regan, S., Waldren, S., Ghosh, B., 2021. A nested drone-satellite approach to monitoring the ecological conditions of wetlands. ISPRS J. Photogramm. Remote Sens. 174 https://doi.org/10.1016/j.isprsjprs.2021.01.012.

Blaschke, T., Hay, G.J., Kelly, M., Lang, S., Hofmann, P., Addink, E., Queiroz Feitosa, R., van der Meer, F., van der Werff, H., van Coillie, F., Tiede, D., 2014. Geographic Object-Based Image Analysis – Towards a new paradigm. ISPRS J. Photogramm. Remote Sens. 87, 180–191. https://doi.org/10.1016/j.isprsjprs.2013.09.014.

Breiman, L., 2001. Random forests. Mach. Learn. 45, 5–32. https://doi.org/10.1023/A:1010933404324.

Colditz, R.R., 2015. An evaluation of different training sample allocation schemes for discrete and continuous land cover classification using decision tree-based algorithms. Remote Sens. 7 (8) https://doi.org/10.3390/rs70809655.

Couwenberg, J., Thiele, A., Tanneberger, F., Augustin, J., Bärisch, S., Dubovik, D., Liashchynskaya, N., Michaelis, D., Minke, M., Skuratovich, A., Joosten, H., 2011. Assessing greenhouse gas emissions from peatlands using vegetation as a proxy. Hydrobiologia 674 (1), 67–89. https://doi.org/10.1007/s10750-011-0729-x.

Cunliffe, A.M., Assmann, J.J., Daskalova, G.N., Kerby, J.T., Myers-Smith, I.H., 2020. Aboveground biomass corresponds strongly with drone-derived canopy height but weakly with greenness (NDVI) in a shrub tundra landscape. Environ. Res. Lett. 15 (12) https://doi.org/10.1088/1748-9326/aba470.

Czapiewski, S., 2022. Assessment of the Applicability of UAV for the Creation of Digital Surface Model of a Small Peatland. Front. Earth Sci. 10 https://doi.org/10.3389/feart.2022.834923.
Dronova, I., 2015. Object-based image analysis in wetland research: A review. Remote Sens. 7 (5) https://doi.org/10.3390/rs70506380.
Fernandez, F., Connolly, K., Crowley, W., Denyer, J., Duff, K., & Smith, G. (2014). Raised Bog Monitoring and Assessment Survey 2013. https://www.npws.ie/sites/default/files/publications/pdf/IWM81_0.pdf.
Fraser, R.H., Olthof, I., Lantz, T.C., Schmitt, C., 2016. UAV photogrammetry for mapping vegetation in the low-Arctic. Arctic Sci. 2 (3) https://doi.org/10.1139/as-2016-0008.
Harris, A., Baird, A.J., 2019. Microtopographic Drivers of Vegetation Patterning in Blanket Peatlands Recovering from Erosion. Ecosystems 22 (5). https://doi.org/10.1007/s10021-018-0321-6.
Jiang, G., Wang, W., 2017. Error estimation based on variance analysis of k-fold cross-validation. Pattern Recogn. 69 https://doi.org/10.1016/j.patcog.2017.03.025.
Kalacska, M., Arroyo-Mora, J.P., Soffer, R.J., Roulet, N.T., Moore, T.R., Humphreys, E., Leblanc, G., Lucanus, O., Inamdar, D., 2018. Estimating Peatland water table depth and net ecosystem exchange: A comparison between satellite and airborne imagery. Remote Sens. 10 (5) https://doi.org/10.3390/rs10050687.
Kelly, J., Kljun, N., Eklundh, L., Klemedtsson, L., Liljebladh, B., Olsson, P.O., Weslien, P., Xie, X., 2021. Modelling and upscaling ecosystem respiration using thermal cameras and UAVs: Application to a peatland during and after a hot drought. Agric. For. Meteorol. 300 https://doi.org/10.1016/j.agrformet.2021.108330.
Kursa, M.B., Rudnicki, W.R., 2010. Feature selection with the boruta package. J. Stat. Softw. 36 (11) https://doi.org/10.18637/jss.v036.i11.
Lees, K.J., Quaife, T., Artz, R.R.E., Khomik, M., Clark, J.M., 2018. Potential for using remote sensing to estimate carbon fluxes across northern peatlands – A review. Sci. Total Environ. 615 https://doi.org/10.1016/j.scitotenv.2017.09.103.
Lehmann, J., Münchberger, W., Knoth, C., Blodau, C., Nieberding, F., Prinz, T., Pancotto, V., Kleinebecker, T., 2016. High-Resolution Classification of South Patagonian Peat Bog Microforms Reveals Potential Gaps in Up-Scaled CH_4 Fluxes by use of Unmanned Aerial System (UAS) and CIR Imagery. Remote Sens. 8 (3), 173. https://doi.org/10.3390/rs8030173.
Lopatin, J., Kattenborn, T., Galleguillos, M., Perez-Quezada, J.F., Schmidtlein, S., 2019. Using aboveground vegetation attributes as proxies for mapping peatland belowground carbon stocks. Remote Sens. Environ. 231 https://doi.org/10.1016/j.rse.2019.111217.
Lovitt, J., Rahman, M.M., McDermid, G.J., 2017. Assessing the Value of UAV Photogrammetry for Characterizing Terrain in Complex Peatlands. Remote Sens. 9 (7), 715. https://doi.org/10.3390/rs9070715.
Mackin, F., Barr, A., Rath, P., Eakin, M., Ryan, J., Jeffrey, R., & Valverde, F. F. (2017). Best practice in raised bog restoration in Ireland. https://www.npws.ie/sites/default/files/publications/pdf/IWM99_RB_Restoration_Best Practice Guidance.pdf.
Manfreda, S., McCabe, M.F., Miller, P.E., Lucas, R., Pajuelo Madrigal, V., Mallinis, G., Ben Dor, E., Helman, D., Estes, L., Ciraolo, G., Müllerová, J., Tauro, F., De Lima, M.I., De Lima, J.L.M.P., Maltese, A., Frances, F., Caylor, K., Kohv, M., Perks, M., Ruiz-Pérez, G., Su, Z., Vico, G., Toth, B., 2018. On the use of unmanned aerial systems for environmental monitoring. Remote Sens. 10 (4) https://doi.org/10.3390/rs10040641.
Millard, K., Richardson, M., 2015. On the importance of training data sample selection in Random Forest image classification: A case study in peatland ecosystem mapping. Remote Sens. 7 (7) https://doi.org/10.3390/rs70708489.
Moore, P.A., Lukenbach, M.C., Thompson, D.K., Kettridge, N., Granath, G., Waddington, J.M., 2019. Assessing the peatland hummock–hollow classification framework using high-resolution elevation models: implications for appropriate complexity ecosystem modeling. Biogeosciences 16 (18), 3491–3506. https://doi.org/10.5194/bg-16-3491-2019.
National Parks and Wildlife Service. (2018). National raised bog special areas of conservation management plan 2017–2022. https://www.npws.ie/sites/default/files/general/national-raised-bog-sac-management-plan-en.pdf.
Olofsson, P., Foody, G.M., Herold, M., Stehman, S.V., Woodcock, C.E., Wulder, M.A., 2014. Good practices for estimating area and assessing accuracy of land change. Remote Sens. Environ. 148, 42–57. https://doi.org/10.1016/j.rse.2014.02.015.
Olofsson, P., Foody, G.M., Stehman, S.V., Woodcock, C.E., 2013. Making better use of accuracy data in land change studies: Estimating accuracy and area and quantifying uncertainty using stratified estimation. Remote Sens. Environ. 129 https://doi.org/10.1016/j.rse.2012.10.031.
Palace, M., Herrick, C., DelGreco, J., Finnell, D., Garnello, A., McCalley, C., McArthur, K., Sullivan, F., Varner, R., 2018. Determining Subarctic Peatland Vegetation Using an Unmanned Aerial System (UAS). Remote Sens. 10 (9), 1498. https://doi.org/10.3390/rs10091498.
Pedregosa, F., Varoquaux, G., Gramfort, A., Michel, V., Thirion, B., Grisel, O., Blondel, M., Prettenhofer, P., Weiss, R., Dubourg, V., Vanderplas, J., Passos, A., Cournapeau, D., Brucher, M., Perrot, M., Duchesnay, É., 2011. Scikit-learn: Machine learning in Python. J. Mach. Learn. Res. 12.
Rahman, M.M., McDermid, G.J., Strack, M., Lovitt, J., 2017. A new method to map groundwater table in peatlands using unmanned aerial vehicles. Remote Sens. 9 (10) https://doi.org/10.3390/rs9101057.
Räsänen, A., Aurela, M., Juutinen, S., Kumpula, T., Lohila, A., Penttilä, T., Virtanen, T., 2020a. Detecting northern peatland vegetation patterns at ultra-high spatial resolution. Remote Sens. Ecol. Conserv. 6 (4) https://doi.org/10.1002/rse2.140.
Räsänen, A., Juutinen, S., Kalacska, M., Aurela, M., Heikkinen, P., Mäenpää, K., Rimali, A., Virtanen, T., 2020b. Peatland leaf-area index and biomass estimation with ultra-high resolution remote sensing. GISci. Rem. Sens. 1–22 https://doi.org/10.1080/15481603.2020.1829377.
Räsänen, A., Juutinen, S., Tuittila, E.S., Aurela, M., Virtanen, T., 2019. Comparing ultra-high spatial resolution remote-sensing methods in mapping peatland vegetation. J. Veg. Sci. 30 (5) https://doi.org/10.1111/jvs.12769.
Räsänen, A., Virtanen, T., 2019. Data and resolution requirements in mapping vegetation in spatially heterogeneous landscapes. Rem. Sens. Environ. 230, 111207 https://doi.org/10.1016/j.rse.2019.05.026.
Riihimäki, H., Luoto, M., Heiskanen, J., 2019. Estimating fractional cover of tundra vegetation at multiple scales using unmanned aerial systems and optical satellite data. Rem. Sens. Environ. 224 https://doi.org/10.1016/j.rse.2019.01.030.
Rydin, H., & Jeglum, J. K. (2013). The Biology of Peatlands. Oxford University Press. https://doi.org/10.1093/acprof:osobl/9780199602995.001.0001.
Schaepman-Strub, G., Limpens, J., Menken, M., Bartholomeus, H.M., Schaepman, M.E., 2009. Towards spatial assessment of carbon sequestration in peatlands: Spectroscopy based estimation of fractional cover of three plant functional types. Biogeosciences 6 (2). https://doi.org/10.5194/bg-6-275-2009.
Siewert, M.B., Olofsson, J., 2020. Scale-dependency of Arctic ecosystem properties revealed by UAV. Environ. Res. Lett. 15 (9) https://doi.org/10.1088/1748-9326/aba20b.
Steenvoorden, J., Limpens, J., Crowley, W., Schouten, M.G.C., 2022. There and back again: Forty years of change in vegetation patterns in Irish peatlands. Ecol. Ind. 145, 109731 https://doi.org/10.1016/j.ecolind.2022.109731.
Virtanen, T., Ek, M., 2014. The fragmented nature of tundra landscape. Int. J. Appl. Earth Obs. Geoinf. 27 (PARTA) https://doi.org/10.1016/j.jag.2013.05.010.
Xu, J., Morris, P.J., Liu, J., Holden, J., 2018. PEATMAP: Refining estimates of global peatland distribution based on a meta-analysis. Catena 160, 134–140. https://doi.org/10.1016/j.catena.2017.09.010.
Yu, Z.C., 2011. Holocene carbon flux histories of the world's peatlands. The Holocene 21 (5), 761–774. https://doi.org/10.1177/0959683610386982.
Yu, Z.C., Loisel, J., Brosseau, D.P., Beilman, D.W., Hunt, S.J., 2010. Global peatland dynamics since the Last Glacial Maximum. Geophys. Res. Lett. 37 (13) https://doi.org/10.1029/2010GL043584.